Materials Transactions, Vol. 47, No. 5 (2006) pp. 1299 to 1302

Visualization of Hydride in Titanium and Titanium-Aluminide by Refraction-Enhanced X-ray Imaging Technique*

Kaoru Mizuno[1], Hiroyuki Okamoto[2], Kentarou Kajiwara[3] and Yoshio Furuya[4]

[1]*Department of Material Science, Faculty of Science and Engineering, Shimane University, Matsue 690-8504, Japan*
[2]*Department of Health Sciences, School of Medicine, Kanazawa University, Kanazawa 920-0942, Japan*
[3]*SPring-8/JASRI, Mikazuki, Hyogo 679-5198, Japan*
[4]*Faculty of Education, Nagasaki University, Nagasaki 852-8521, Japan*

Refraction-enhanced X-ray imaging method using extremely parallel X-ray beams from a so-called third generation synchrotron radiation source was applied to observe titanium-hydride in titanium and titanium-aluminide polycrystals. Hydride in titanium was formed by an annealing in 1 atm hydrogen gas and electrolytic-charging for cross-sectional observation. Although the hydride in titanium cannot be observed by conventional radiography that utilizes absorption of X-rays, we visualized a high-contrast projection image of hydride using refraction-contrast radiography. This is a promising new technique for non-destructive inspection in bulk material systems with only small differences between refraction indexes such as hydride in titanium. [doi:10.2320/matertrans.47.1299]

(Received December 6, 2005; Accepted February 24, 2006; Published May 15, 2006)

Keywords: *titanium, hydride, refraction-enhanced X-ray imaging, phase contrast, synchrotron radiation*

1. Introduction

There have been a number of investigations of the interaction between metals and hydrogen atoms in order to solve problems such as hydrogen embrittlement in steel or hydrogen-storing materials. However, many investigations in metal physics deal with indirect detection techniques for hydrogen in solids such as thermal desorption or penetration of hydrogen atoms. A few studies on direct observation of hydride in metals by electron microscopy have been reported; however, this observation was limited to only local areas and conditions.[1)] As yet there have been no reports on direct observation of shape, distribution, formation and decomposition of hydride in bulk metals under highly concentrated hydrogen atmospheres. Although titanium and its alloys are promising materials for preserving hydrogen, until now it has been impossible to visualize the hydride in titanium with non-destructive methods.

Imaging techniques utilizing high-energy X-rays such as projection radiography and tomography have been used for many years to non-destructively observe the image contrast of the internal structures of objects in material science, biology and medicine.[2)] In conventional radiography, X-rays that pass through an object along different paths are differently absorbed, and the intensity pattern of the emerging beam records the distribution of absorbing materials within the sample. An alternative approach is phase-contrast radiography, which instead records variations in the phase of the emerging radiation.[3)] Such an approach offers improved contrast sensitivity, especially when imaging weakly absorbing samples.[4)] Since the interaction cross section of the X-ray phase shift is about a thousand times larger the that of absorption, an extremely high sensitivity is attained by X-ray phase imaging, enabling the observation of material systems with light elements.[5)] This technique, phase contrast X-ray microscopy, is successfully progressing now in the soft X-ray region because of application for diagnostic tools in medicine and biological X-ray microscope.[6)] For imaging in the hard X-ray region, a extreme parallelism is needed in order to enhance the contrast and to be able to resolve phase variations across the beam. Because of the extremely parallel X-ray beam provided by a so-called third-generation synchrotron radiation source such as SPring-8, it is possible to realize phase-contrast imaging directly from the sample in transmission geometry.[7–9)] By the way, refraction is always accompanied by the spatially variant phase shift since waves propagate in the direction perpendicular to the wave front. So, phase contrast imaging technique is also called as refraction contrast imaging method.

Therefore, present work was planned and performed with the aim of confirming the visualization of titanium-hydride in titanium and titanium-aluminide by the most simple X-ray refraction contrast technique, refraction-enhanced X-ray imaging method (propagation-based method).[10)]

2. Experimental Procedures

The specimens used in this investigation were polycrystals of α-titanium (99.99 at%) and titanium-aluminide. The sample's dimensions were approximately $1.0 \times 10 \times 20$ mm. After annealing of 800°C in vacuum for 1 h, the three titanium specimens were annealed at 560°C in hydrogen gas at 1 atom, and the annealing times were 0 (non hydrogen annealing), 1200, 3600 s, respectively. To observe a cross section of specimen, we also prepared another specimen with hydride deposited on the surface by an electrolytic-charge. The charge was carried out in 1-N sulfuric acid at room temperature. The current density and charging time were 5 mA/mm^2 and 20 h, respectively. The specimen was cut into a 1-mm thick slice for cross-sectional observation. After observation of the cross-section, we annealed the specimen at 550°C in a vacuum for 1 h in order to decompose the hydride on the surface, and observed it again. Titanium-aluminide

*This Paper was Originally Published in Japanese in J. JILM **55** (2005) 678–681.

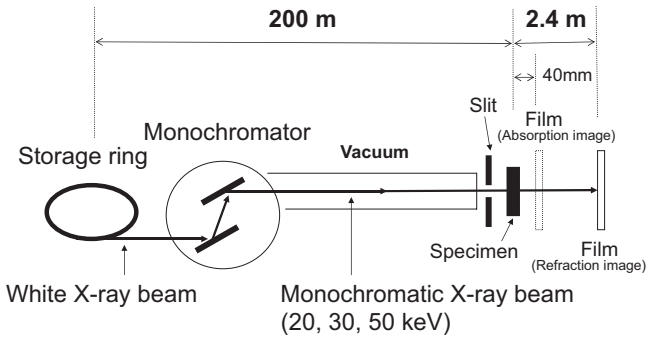

Fig. 1 Schematic diagram of the beam line and experimental setup for refraction-enhanced X-ray imaging method. The experiment was performed at beamline BL20B2 (Bio-medical imaging station) of SPring-8. The images were recorded with a long specimen-to-detector distance (2.4 m) for the refraction images in addition to a short distance (40 mm) for the absorption images.

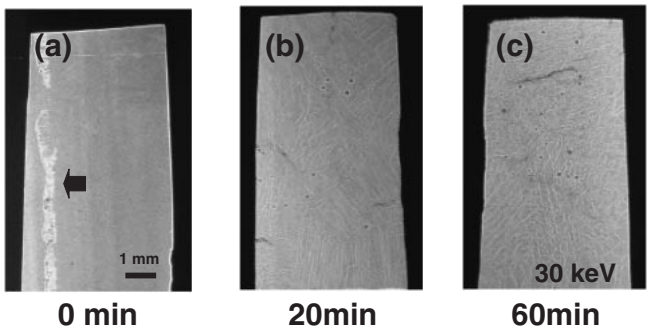

Fig. 2 X-ray refraction-contrast images of titanium specimen taken with 30 keV X-ray. (a) Specimen annealed in vacuum at 850°C for 3600 s, (b) annealed in hydrogen gas at 560°C for 1200 s and (c) annealed in hydrogen gas at 560°C for 3600 s.

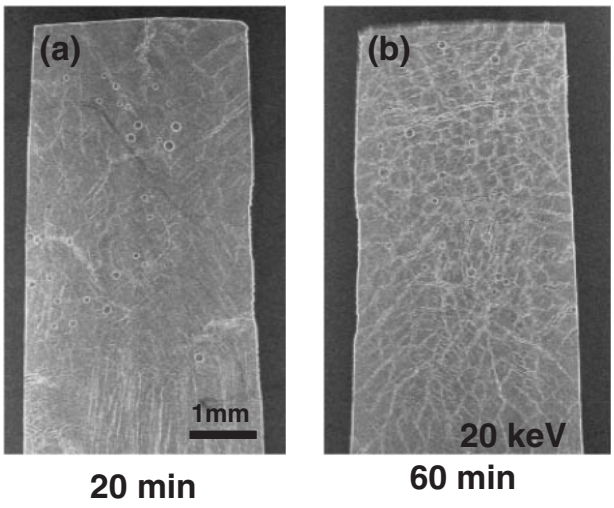

Fig. 3 X-ray refraction-contrast images of titanium specimen taken with 20 keV X-ray. (a) Specimen annealed in hydrogen gas at 560°C for 1200 s and (b) annealed in hydrogen gas at 560°C for 3600 s. Hydride was observed as white lines and was formed along lattice defects such as grain boundary.

specimen was also prepared by an electrolytic-charge in a similar way of the titanium. The cross-section of aluminide specimens was observed before and after the electrolytic-charging.

Present experiment was performed at beamline BL20B2 (Bio-medical imaging station) of SPring-8 in Japan. Schematic diagram of the beam line and experimental setup is shown in Fig. 1. The X-ray energy used in this experiment was 20, 30 and 50 keV. The image contrast and the resolution due to refraction depend on energy of X-ray.[11] Thus, it is necessary to optimize the X-ray energy to obtain maximum image contrast and high special resolution. The images were recorded with a long specimen-to-detector distance (2.4 m) for the refraction images in addition to a short distance (40 mm) for the absorption images. The exposure times of the refraction images were 120 s. for 20 keV, 20∼30 s. for 30 keV and 12 s. for 50 keV X-ray. Images were stored on manmographic film (Kodak Min-R 2000) with a spatial resolution of about 10 μm.

3. Results and Discussion

Figure 2 shows refraction-enhanced imaging photographs of titanium without (a) and with hydride (b), (c) taken with a long specimen-to-detector distance (2.4 m) using 30 keV X-ray. The annealing times in hydrogen gas of the specimens shown in Figs. 2(a), 2(b) and 2(b) were 0 (non-annealing), 1200 and 3600 s, respectively. Large cracks, indicated by arrows, marked by rolling are clearly discernible in Fig. 2(a). These surface cracks were also observed through an optical microscope. Some porosity showing white ring and black concentric circle images are also observed in Figs. 2(b) and (c). In contrast with the specimen shown in Fig. 2(a), these crystals were not rolled in the preparing process. The images obtained using the refraction-enhanced imaging technique is sensitive to the presence of air in the specimen because of the large difference between the refractive indexes of titanium and air. In addition to the porosity images, there are many line images with white contrast in Figs. 2(b) and (c), but we could not observe the white line images in Fig. 2(a). The number density of white lines is dependent on the annealing time in hydrogen gas. Then, we founded that the white contrast image originated by refraction of hydride and the images were not observed in the specimen annealed in vacuum.

Figure 3 shows an X-ray refraction-enhanced image of the hydrogen-annealed specimen shown in Figs. 2(b) and (c) taken with 20 keV X-ray. Hydride was observed as white lines and probably formed along lattice mismatch such as grain boundary. Figure 3 indicates that the refraction image taken with 20 keV X-ray shows high-contrast projection images of hydride.

Figure 4 also shows an X-ray refraction-enhanced image of the hydrogen-annealed specimen shown in Figs. 2(b) and (c) taken with 50 keV X-ray. Photographs taken with 50 keV X-ray show lower contrast projection image of hydride rather than those with 20 and 30 keV X-ray. However, small cracks were clearly observed in Fig. 4(b). The cracks were observed along the hydride seen in Fig. 3(b). Deposition of hydride generated the cracks.

Figure 5 shows an X-ray image of the hydrogen-annealed specimen shown in Figs. 3(b) and 4(b) taken with 30 keV X-ray under absorption contrast conditions with a short speci-

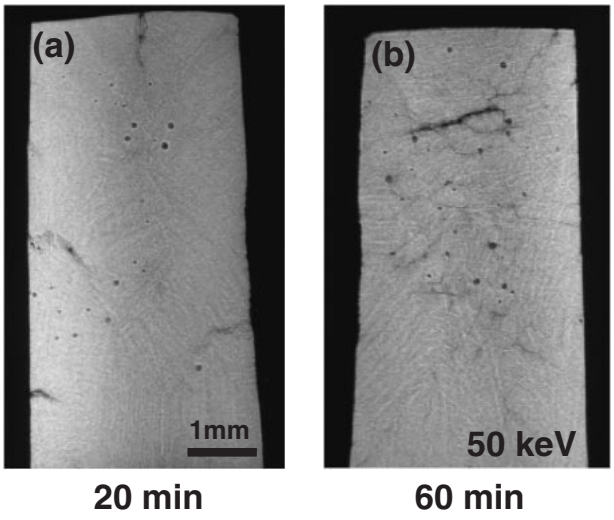

Fig. 4 X-ray refraction-contrast images of titanium specimen taken with 50 keV X-ray. (a) Specimen annealed in hydrogen gas at 560°C for 1200 s and (b) annealed in hydrogen gas at 560°C for 3600 s. Thin cracks were clearly observed in addition to the hydride with week contrast. They were generated by segregation of hydride.

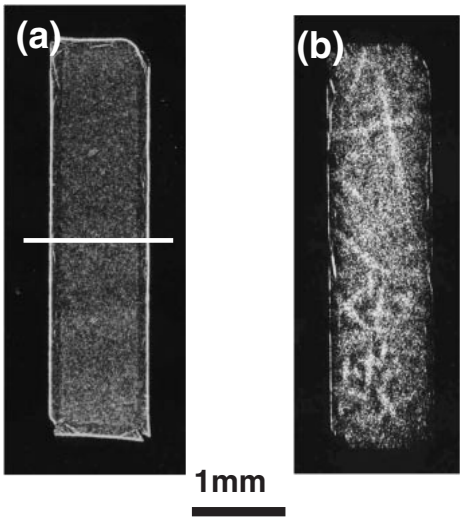

Fig. 6 X-ray refraction-contrast images through a cross-section of titanium charged by an electrolytic method; (a) image was taken after the hydrogen charge and (b) taken after annealing at 550°C in a vacuum to decompose the hydride. The circumference of the specimen with hydride has white and black contrast image originated by surface layer of hydride.

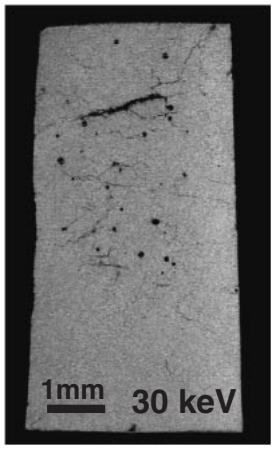

Fig. 5 X-ray absorption image of the hydrogen-annealed titanium at distance 40 mm. We could not observe the line images with white contrast seen in Figs. 3(b) and 4(b). This result indicates that the white contrast image is due to the refraction of X-rays by the hydride in specimen.

men-to-detector distance (40 mm). In this image, we could not observe the line images with white contrast seen in Figs. 3(b) and 4(b). This result indicates that the white contrast image is due to the refraction of X-rays by the hydride in specimen.

It is difficult to explain the observed images of hydrides by refraction; the hydrides have complicated shapes because they were formed by the hydrogen-gas annealing at high temperature (560°C). To confirm that the image does indeed show the hydride in titanium, we also observed a cross-section of the specimen covered with surface hydride using 30 keV X-ray. Figure 6(a) shows a cross-sectional profile of the specimen charged by the electrolytic method described previous section. The circumference of the specimen has white and black contrast images. Because hydrogen-charging of this specimen was carried out at room temperature, in contrast to the hydrogen gas annealing, hydrogen atoms could not diffuse into the crystal on account of the high migration energy of hydrogen (0.49 eV).[12] Thus, hydrides were formed on the surface of the specimen. After X-ray observation, this specimen was annealed at 550°C for 3600 s in a vacuum. The annealing is to decompose the hydride into hydrogen and titanium metal.[13] Figure 6(b) shows a cross-sectional profile of the annealed specimen, where we can clearly observe the inner structures, as opposed to Fig. 6(a), where we cannot. However, most of the refraction contrast image of hydride at the specimen surface shown in Fig. 6(a) disappeared. Therefore, we confirmed that refraction contrast image shown in Fig. 6(a) originated from the titanium-hydride deposited on the surface. Some of the oblique and thick lines are acicular α-phase (secondary α-phase), and the hydrogen in the titanium enhanced the image contrast of the α-phase. Almost all the hydrogen atoms decomposed from hydride may desorb from the specimen during vacuum annealing but small amount of the atoms diffuse into the crystal lattice. They will be trapped at strain field of acicular α-phase and formed hydride near the α-phase again. The hydride enhanced image contrast of acicular α-phase as shown in Fig. 6(b).

The principle of generating the refraction-contrast in Fig. 6(a) is schematically shown in Fig. 7. The intensity distribution in Fig. 7 corresponds to the contrast along the white line shown in Fig. 6(a). Since the refraction index of titanium for X-rays is greater than that of titanium hydride, the distribution of titanium acts as a converging lens. Note that the direction of deflection is not the same as that for visible light because the index of refraction for X-rays is slightly smaller than unity. In this figure, the inward deflection causes a white and black fringe at the edge of the specimen as shown in X-ray intensity distribution. In Fig. 6(a), width of white band in the fringe was about one third of that of the black band. This may be attributed to that the inward deflection angle is varied by the concentration of hydride. Width of the fringe may vary according to the

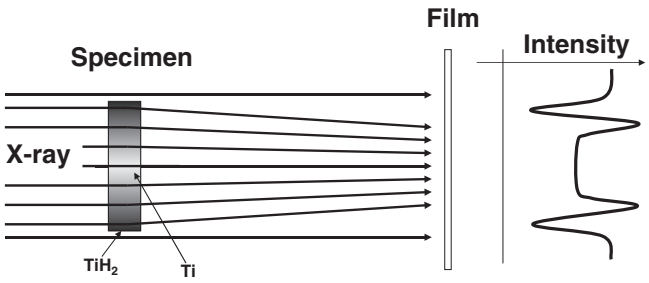

Fig. 7 Schematic plan view of generation of refraction contrast. The direction of the X-ray is slightly deflected at the interface. The intensity distribution is corresponding to the contrast along the white line shown in Fig. 6(a).

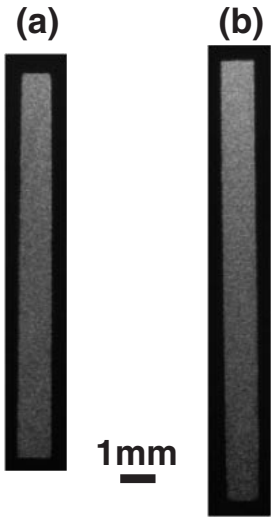

Fig. 8 X-ray refraction-contrast images through a cross-section of titanium-aluminum alloy charged by an electrolytic method; (a) image was taken before the hydrogen charge and (b) taken after charging for 48 h. There are no hydrides at the surface in contrast with Fig. 6(a).

specimen-to-film distance. However, we could not take another photograph with difference distance in the present experiment.

Figure 8 shows X-ray refraction-enhanced images of the cross-section of titanium-aluminide specimens before (a) and after (b) the electrolytic-charging for 20 h. Many small grains were observed in the specimen as shown in Figs. 8(a) and (b), while the image of grains was not observed in the pure titanium crystals. This image probably originated from the lamella structure in the alloy.[14] Furthermore, in contrast with titanium, refraction-contrast images of hydride were not observed in titanium-aluminum alloy seen in Fig. 8(b). It seems that aluminum atoms prevent the hydride formation. Detailed studies of the phenomena in the aluminide are now in progress.

In summary, we confirmed that titanium-hydride in titanium can be visualized by an X-ray refraction-enhanced imaging technique despite the small difference between refraction indexes. This refraction-enhanced imaging appears to be a promising new technology for non-destructive inspection of bulk materials.

The synchrotron radiation experiments were performed at SPring-8 with the approval of the Japan Synchrotron Radiation Research Institute (JASRI) (Proposal No. J01B20B2-0506N).

REFERENCES

1) K. Aoyagi, E. P. Torres, T. Suda and S. Ohnuki: J. Nuclear Materials **283–287** (2000) 876–879.
2) L. V. Azaroff, B. Kaplow, N. Kato, P. Weiss, W. Wilson and S. Young: *X-ray Diffraction*, (McGraw-Hill, 1974) pp. 180–186.
3) V. A. Somenkov, A. K. Tkalch and S. Sh. Shil'shtein: Aov. Phys. Tech. Phys. **36** (1991) 1309–1311.
4) J. Kirz: Q. Rev. Biophys. **28** (1995) 33–130.
5) A. Momose: Jpn. J. Appl. Phys. **44** (2005) 6355–6367.
6) A. Snigirev, I. Snigreva, V. Kohn, S. Kuzunetsov and I. Schelokov: Rev. Sci. Instrum. **66** (1995) 5486–5492.
7) D. C. Chapman, W. Thomlinson, R. E. Johnston, D. Washburn, E. Pisano, N. Gmur, Z. Zhang, R. Menk, F. Arfel and D. Sayers: Phys. Med. Biol. **42** (1997) 2015–2025.
8) K. Kagoshima, Y. Tsusaka, K. Yokoyama, K. Takai, S. Takeda and J. Matsui: Jpn. J. Appl. Phys. **38** (1999) L470–L472.
9) T. Weitkamp, M. Drakopoulos, W. Leitenberger, C. Raven, C. Schroer, A. Simionovici and A. Snigirev: *X-RAY MICROSCOPY*, (ed. W. Meyer-Ilse, T. Warwick and A. Attwood), American Institute of Physics, (2000) pp. 424–427.
10) N. Yagi, Y. Suzuki, K. Umetani, Y. Kohmura and K. Yamasaki: Med. Phys. **26** (1999) 2190–2193.
11) Y. Suzuki, N. Yagi, K. Umetani, Y. Kohmura and K. Yamasaki: SPIE Proceedings **3770** (1999) 13–21.
12) H. Wipf, B. Kappesser and R. Werner: J. Alloys and Compounds **310** (2000) 190–195.
13) A. Takasaki, Y. Furuya, K. Ojima and Y. Taneda: J. Alloys and Compounds **224** (1995) 269–273.
14) M. Yamaguchi, H. Inui and K. Ito: Acta Mater. **48** (2000) 307–322.